X-ray Crystallographic Analyses of Inhibitor and Substrate Complexes of Wild-type and Mutant 4-Hydroxybenzoyl-CoA Thioesterase*

James B. Thoden‡, Hazel M. Holden‡§, Zhihao Zhuang¶, and Debra Dunaway-Mariano¶‖

From the ‡Department of Biochemistry, University of Wisconsin, Madison, Wisconsin 53706-1544 and the ¶Department of Chemistry, University of New Mexico, Albuquerque, New Mexico 87131

The metabolic pathway by which 4-chlorobenzoate is degraded to 4-hydroxybenzoate in the soil-dwelling microbe *Pseudomonas* sp. strain CBS-3 consists of three enzymes including 4-hydroxybenzoyl-CoA thioesterase. The structure of the unbound form of this thioesterase has been shown to contain the so-called "hot dog" fold with a large helix packed against a five-stranded antiparallel β-sheet. To address the manner in which the enzyme accommodates the substrate within the active site, two inhibitors have been synthesized, namely 4-hydroxyphenacyl-CoA and 4-hydroxybenzyl-CoA. Here we describe the structural analyses of the enzyme complexed with these two inhibitors determined and refined to 1.5 and 1.8 Å resolution, respectively. These studies indicate that only one protein side chain, Ser[91], participates directly in ligand binding. All of the other interactions between the protein and the inhibitors are mediated through backbone peptidic NH groups, carbonyl oxygens, and/or solvents. The structures of the enzyme-inhibitor complexes suggest that both a hydrogen bond and the positive end of a helix dipole moment serve to polarize the electrons away from the carbonyl carbon of the acyl group, thereby making it more susceptible to nucleophilic attack. Additionally, these studies demonstrate that the carboxylate group of Asp[17] is ∼3.2 Å from the carbonyl carbon of the acyl group. To address the role of Asp[17], the structure of the site-directed mutant protein D17N with bound substrate has also been determined. Taken together, these investigations suggest that the reaction mechanism may proceed through an acyl enzyme intermediate.

The soil-dwelling microbe *Pseudomonas* sp. strain CBS-3 is capable of surviving on 4-chlorobenzoate as its sole source of

carbon (1). The metabolic pathway by which 4-chlorobenzoate is degraded to 4-hydroxybenzoate in this organism is outlined in Scheme 1 (2). The focus of this paper, 4-hydroxybenzoyl-CoA thioesterase, catalyzes the third step in this degradative pathway, namely the hydrolysis of the thioester moiety in 4-hydroxybenzoyl-CoA to yield 4-hydroxybenzoate and CoA. Previous x-ray crystallographic studies of this thioesterase have revealed that each subunit of the homotetrameric enzyme contains a five-stranded anti-parallel β-sheet and three major α-helices as shown in Fig. 1 (3). The molecular architecture of this thioesterase is topologically equivalent to that observed in β-hydroxydecanoyl thiol ester dehydrase from *Escherichia coli* and has been referred to as the "hot dog" fold (4). In the case of the *E. coli* dehydrase, the functional unit is a dimer in which the two active sites are located at the subunit-subunit interface. The recently reported structure of the long chain acyl-CoA thioesterase II from *E. coli* shows that in the case of this dimeric protein, each monomer is composed of two hot dog folds connected by a linker region (5). In addition to possessing similar molecular motifs, all three enzymes recognize a pantetheine-linked acyl-thioester substrate: acyl-CoA in the cases of the two thioesterases and acyl carrier protein in the case of the dehydrase. Despite similarities in their substrates and three-dimensional architectures, these enzymes do not share significant amino acid sequence identities. Recent BLAST searches, however, have identified unique, nonoverlapping sets of homologs for each of these enzymes, indicating that this hot dog superfamily may be both vast and ancient. Most likely this superfamily is composed of smaller protein families, which have diverged to such a point that detectable amino acid sequence homologies are no longer present.

The first reported structure of the *Pseudomonas* sp. strain CBS-3 thioesterase was that of the unbound enzyme (3). In light of the structural similarity between this thioesterase and β-hydroxydecanoyl thiol ester dehydrase complexed with 3-decynoyl-*N*-acetylcysteamine, a model of 4-hydroxybenzoyl-CoA was positioned into the thioesterase putative active site (3). On the basis of this model building study, it was postulated that Asp[17] was important for the proper positioning of a water molecule required for nucleophilic attack on the thioester carbonyl carbon of the substrate. To further characterize the functional groups on the enzyme that participate in substrate binding and catalysis, recent efforts have been directed toward the synthesis of tight binding substrate analogs resistant to catalyzed hydrolysis. Two such inhibitors, 4-hydroxyphenacyl-CoA and 4-hydroxybenzyl-CoA, have now been identified and are shown in Scheme 2. As described here, subsequent x-ray crystallographic analyses of these two enzyme-inhibitor complexes further indicate a key role for Asp[17] in the reaction mechanism of the thioesterase. To test the presumed catalytic role of this

§ To whom correspondence may be addressed: Dept. of Biochemistry, 433 Babcock Dr., University of Wisconsin, Madison, WI 53706-1544. Tel.: 608-262-4988; Fax: 608-262-1319; E-mail: Hazel_Holden@biochem.wisc.edu.

‖ To whom correspondence may be addressed. Tel.: 505-277-3383; Fax: 505-277-6202; E-mail: dd39@unm.edu.

[A] 4-chlorobenzoyl CoA ligase

[B] 4-chlorobenzoyl CoA dehalogenase

[C] 4-hydroxybenzoyl CoA thioesterase
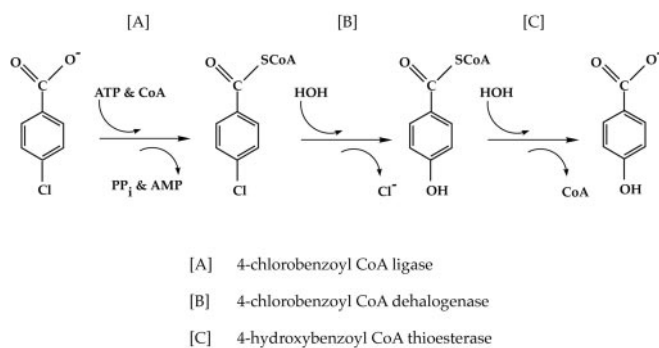
SCHEME 1

aspartate, site-directed mutagenesis experiments have been conducted whereby it has been substituted with an asparagine residue. At 25 °C and pH 7.5, the k_{cat} of this mutant protein is 5×10^{-4} s^{-1} compared with 15 s^{-1} measured for the wild-type enzyme.[1] This slow activity allowed the mutant enzyme D17N to be co-crystallized with its substrate, 4-hydroxybenzoyl-CoA. The high resolution x-ray structures of the complexes between wild-type protein and 4-hydroxyphenacyl-CoA, wild-type protein and 4-hydroxybenzyl-CoA, and D17N mutant protein and 4-hydroxybenzoyl-CoA are described here. Taken together, these enzyme-inhibitor (or substrate) complexes provide a three-dimensional understanding of substrate binding and catalysis in this thioesterase.

EXPERIMENTAL PROCEDURES

Enzyme Purification and Crystallization—Wild-type *Pseudomonas* sp. strain CBS-3 4-hydroxybenzoyl-CoA thioesterase was purified as described previously (7). The D17N mutant protein was prepared and purified according to Zhuang *et al.*[1] Crystallization conditions were tested at both room temperature and at 4 °C with a sparse matrix screen composed of 144 conditions. The protein solution was concentrated to 14 mg/ml and contained 10 mM HEPES (pH 7.0), 200 mM KCl, and 5 mM 4-hydroxyphenacyl-CoA. The best crystals grew from 10% polyethylene glycol 8000, 2% Me$_2$SO, and 100 mM succinate (pH 5.0) at room temperature. Larger crystals of dimensions $0.25 \times 0.25 \times 0.35$ mm were produced by macro-seeding into batch experiments containing 2–4% polyethylene glycol 8000, 200 mM KCl, and 100 mM succinate (pH 5.0). These crystals belonged to space group I222 with unit cell dimensions of $a = 49.4$ Å, $b = 54.6$ Å, and $c = 93.1$ Å and contained one subunit in the asymmetric unit. Macro-seeding techniques under similar conditions were used to obtain isomorphous crystals grown in the presence of 4-hydroxybenzyl-CoA.

Crystals of the D17N mutant protein in complex with the substrate 4-hydroxybenzoyl-CoA were first identified from a sparse matrix screen and "optimized" in batch by macro-seeding into droplets containing 8–10% polyethylene glycol 5000-*O*-methyl ether, 200 mM KCl, 100 mM MES[2] (pH 6.0), and 1 mM substrate with the protein concentration at 5 mg/ml. These crystals were difficult to grow and achieved, at best, maximal dimensions of $0.075 \times 0.075 \times 0.1$ mm. Like the wild-type enzyme, the D17N mutant protein crystallized in the space group I222 with unit cell dimensions of $a = 49.4$ Å, $b = 54.6$ Å, and $c = 93.1$ Å and one subunit in the asymmetric unit.

X-ray Data Collection and Processing—Prior to x-ray data collection, the wild-type thioesterase crystals in complex with 4-hydroxyphenacyl-CoA or 4-hydroxybenzyl-CoA were transferred to a cryoprotectant solution composed of 20% polyethylene glycol, 250 mM KCl, 20% ethylene glycol, and 100 mM succinate (pH 5.0). This solution also included the relevant CoA inhibitor at a concentration of 5 mM. The crystals were suspended in 20-μm nylon loops and flash cooled to −150 °C in a nitrogen gas stream. Because of their small size, the D17N protein crystals were mounted in quartz capillary tubes, and the x-ray data were collected at 4 °C. X-ray data from the wild-type enzyme-4-hydroxy-

phenacyl-CoA complex crystals were collected at the Structural Biology Center beam line 19-ID at the Advanced Photon Source (Argonne National Laboratories) and reduced with HKL2000 (8). X-ray data from the wild-type protein/4-hydroxybenzyl-CoA and the D17N mutant protein/4-hydroxybenzoyl-CoA crystal complexes were collected with a HiStar (Bruker AXS) area detector system using CuKα radiation from a Rigaku RU200 x-ray generator operated at 50 kV and 90 mA and equipped with Supper "long" mirrors. The x-ray data were processed with the software package SAINT (Bruker AXS, Inc.) and internally scaled with XSCALIBRE.[3] Relevant x-ray data collection statistics for all protein complexes are presented in Table I.

Structure Determination and Refinement—The three structures described here were solved via molecular replacement methods using the software package AMORE (9) and the previously solved unbound thioesterase as the search model (3). The software package TNT was employed for least squares refinements (10). All model building was done via TURBO (11). Relevant refinement statistics are given in Table II.

Synthesis of Inhibitors—4-Hydroxyphenacyl-CoA was prepared as described previously (12). 4-Hydroxybenzyl-CoA was synthesized according to the following procedure. Under N$_2$ protection, 30 μl of 4-(chloromethyl)phenyl acetate and 30 mg of CoA were allowed to react in a 1:1 H$_2$O/tetrahydrofuran solution for 12 h at room temperature. During this period the pH of the reaction solution was maintained between 7.5 and 8.0 by adding 0.1 M LiOH. The pH was then adjusted to 11 with 1 M KOH to facilitate the hydrolysis of the acetate group. After 1 h the pH was reduced to 7.5, and the solution was extracted with two 10-ml portions of ethyl acetate. The aqueous layer was concentrated by lyophilization. The concentrate was loaded onto a 120×2.5-cm Sephadex G-25 (Amersham Biosciences) column and eluted with deionized water at a flow rate of 0.25 ml/min. The fractions containing 4-hydroxybenzyl-CoA were collected, analyzed by high pressure liquid chromatography, pooled, and concentrated. The yield of pure 4-hydroxybenzyl-CoA was 23 mg (70%). The UV spectrum was as follows (in 50 mM HEPES, pH 7.5): $\lambda_{max} = 260$ nm, $\epsilon_{260} = 16,400$ M^{-1} cm^{-1}. ^{1}H NMR (D$_2$O, pH 6.0): δ 0.52 (s, ^{3}H, 11″), 0.68 (s, ^{3}H, 10″), 2.24 (t, 2H, $J = 6.5$ Hz, 6″), 2.33 (t, 2H, $J = 7.0$ Hz, 9″), 3.07 (t, 2H, $J = 7.0$ Hz, 8″), 3.27 (t, 2H, $J = 7.0$ Hz, 5″), 3.38 (d, 1H, $J = 9.5$ Hz, 1″), 3.46 (s, 2H, benzyl methylene H), 3.64 (d, 1H, $J = 9.5$ Hz, 1″), 4.02 (s, 1H, 3″), 5.97 (d, 1H, $J = 7.0$ Hz, 1′), 6.61 (d, 2H, $J = 8.5$ Hz, aromatic H), 6.96 (d, 2H, $J = 8.5$ Hz, aromatic H), 8.04 (s, 1H, 2), 8.36 (s, 1H, 8). ^{13}C NMR (D$_2$O pH 6.0) δ 20.8 (CH$_3$, 11″), 23.5 (CH$_3$, 10″), 32.3 (CH$_2$, benzyl methylene C), 37.1 (CH$_2$, 6″), 38.1 (C, 2″), 41.1 (CH$_2$, 5″), 68.2 (CH$_2$, 5′), 75.1 (CH$_2$, 1″), 76.7 (CH, 2′ and 3′), 86.5 (CH, 4′), 89.1 (CH, 1′), 119.1 (aromatic C-H), 132.9 (aromatic C-H), 142.5 (CH, 8), 152.0 (C, 4), 155.5 (CH, 2), 159.2 (C, 6), 176.5 (C = O, 7″), 177.4 (C = O, 4″).

Inhibitor Binding—The binding affinities of the 4-hydroxyphenacyl-CoA and 4-hydroxybenzyl-CoA were evaluated by measuring the competitive inhibition constant K_i (wild-type thioesterase only) and by measuring the dissociation constant K_d via fluorescence spectral titration (wild-type and D17N thioesterase). For measurement of the competitive inhibition constants, the initial velocity of thioesterase catalyzed hydrolysis of 4-hydroxybenzoyl-CoA was measured using the 4-hydroxybenzoate hydroxylase-coupled spectrophotometric assay described in Ref. 7. The reactions were carried out in 50 mM HEPES (pH 7.5 at 25 °C) containing wild-type 4-hydroxybenzoyl-CoA thioesterase (0.004 μM), 0.1 mM NADPH, 0.1 mM FAD, 0.5 unit/ml 4-hydroxybenzoate hydroxylase, and varying concentrations of 4-hydroxybenzoyl-CoA (2–38 μM) with (0.6–2.5 μM) or without inhibitor. For all measurements, the initial velocity data were analyzed using Equation 1 and the computer program KinetAsyst (IntelliKinetics, State College, PA).

$$V = V_{max}[S]/[K_m(1 + [I]/K_i) + [S]] \qquad (\text{Eq. 1})$$

where V is the initial velocity, V_{max} is the maximum velocity, [S] is the substrate concentration, K_m is the Michaelis constant, [I] is the inhibitor concentration, and K_i is the inhibition constant. The k_{cat} was calculated from V_{max}/[E], where [E] is the total enzyme concentration.

Ligand Binding—A FluoroMax-2 fluorometer was employed in protein fluorescence quenching experiments aimed at measuring the binding constants of 4-hydroxybenzoyl-CoA, 4-hydroxybenzyl-CoA, and 4-hydroxyphenacyl-CoA with wild-type protein and/or with the D17N mutant thioesterase. The fluorescence spectrum of wild-type and D17N 4-hydroxybenzoyl-CoA thioesterase (0.5 μM) in 50 mM HEPES, 0.2 M KCl, 1 mM dithiothreitol (pH 7.5 at 25 °C) resulting from 290 nm

FIG. 1. **Ribbon representation of one subunit of 4-hydroxybenzoyl-CoA thioesterase.** All of the figures were prepared with the software package MOLSCRIPT (6). *Cterm*, C terminus; *Nterm*, N terminus.

SCHEME 2
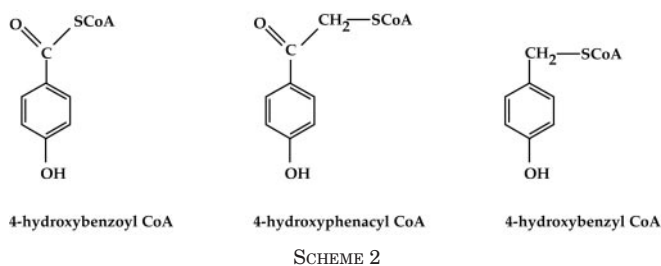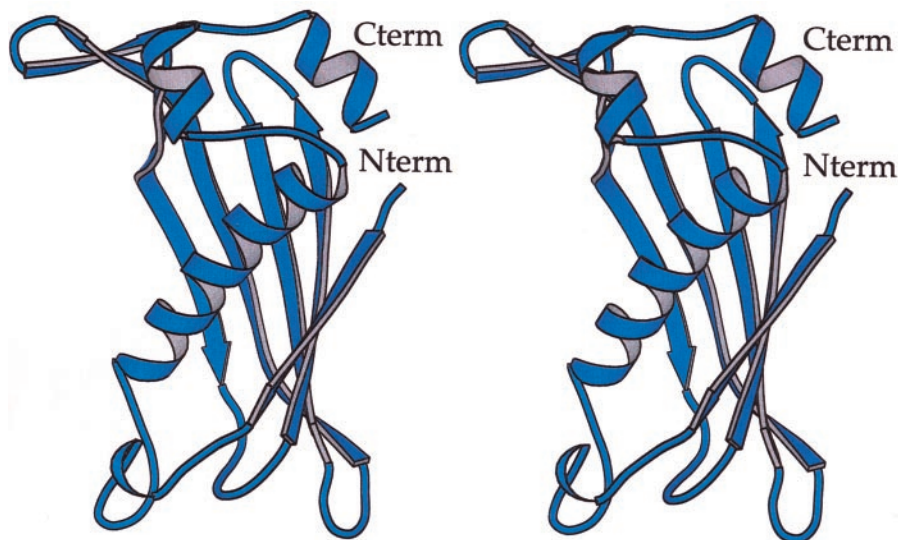
excitation is characterized by an emission maximum at 334 nm. For a typical titration experiment, 1-μl aliquots of ligand were added to a 1 ml solution of 0.5 μM of thioesterase, and the fluorescence intensity measured at 334 nm following each addition. The fluorescence data, collected at ligand concentrations ranging from 0 to 12 μM, were fitted to Equation 2 (13) using the Kaleida Graph computer program for nonlinear regression analysis.

$$\Delta F/F_0 = (\Delta F_{max}/F_0 \cdot [\text{E}])\{(K_d + [E] + [S])$$

$$- \sqrt{(K_d + [E] + [S])^2 - 4[E][S]\}/2} \quad \text{(Eq. 2)}$$

where [S] is the total ligand concentration, [E] is the total enzyme concentration, K_d is the apparent dissociation constant of the enzyme-ligand complex, ΔF is the observed change in fluorescence intensity, $\Delta F_{\max}$ is the maximum change in fluorescence intensity, and F_o is the initial fluorescence intensity.

RESULTS AND DISCUSSION

Thermodynamic Properties of the Enzyme-Ligand Complexes—The fluorescence spectrum of wild-type and D17N 4-hydroxybenzoyl-CoA thioesterase resulting from 290 nm Trp excitation is characterized by an emission maximum at 334 nm. The enzyme contains four Trp residues at positions 23, 30, 47, and 87. Both Trp[23] and Trp[47] are located in the active site. Binding of 4-hydroxybenzyl-CoA produces a 37% reduction in fluorescence intensity caused by static quenching. Strikingly, binding of 4-hydroxybenzoyl-CoA and 4-hydroxyphenacyl-CoA results in 90% reduction in fluorescence intensity, suggesting that an additional mechanism of fluorescence quenching is operative. The 4-hydroxybenzyl-CoA ligand (in buffer or bound to the thioesterase) does not absorb beyond 280 nm, but the 4-hydroxyphenacyl-CoA and 4-hydroxybenzoyl-CoA ligands do, especially when bound to the enzyme. This long wavelength absorption (290–380 nm) introduces a significant filter effect. Such an effect may influence the K_d values obtained from fluorescence titration experiments. Thus, the apparent K_d values reported for 4-hydroxybenzyl-CoA in Table III are expected

to be true to the actual dissociation constants, whereas the apparent K_d values reported for 4-hydroxyphenacyl-CoA and 4-hydroxybenzoyl-CoA may be smaller than the true dissociation constants.

The binding constants of the two substrate analogs were also evaluated by measuring their competitive inhibition constants (Table III). In these measurements, the very small K_m value of the substrate introduces uncertainty into the K_i value extracted, despite the low error obtained in data fitting. Our interpretation of the binding constants obtained by the two independent methods is simply that the substrate and inhibitor ligands bind to the thioesterase with high affinity ($K_d = \sim 1 \mu$M) and that mutation of Asp[17] to an asparagine residue does not impair this tight binding.

Overall Structure of the Thioesterase Complexes—The structures of the wild-type thioesterase complexed with either 4-hydroxyphenacyl-CoA or 4-hydroxybenzyl-CoA were determined to 1.5 and 1.8 Å resolutions, respectively. The structure of the D17N mutant protein with bound substrate was determined to a nominal resolution of 2.8 Å. As an example of coordinate quality, a Ramachandran plot for the thioesterase-4-hydroxyphenacyl-CoA complex is shown in Fig. 2*a*, and the electron density corresponding to the bound ligand is displayed in Fig. 2*b*. Only two residues adopt dihedral angles significantly outside of the allowed regions of the Ramachandran plot, namely Asp[75] and Arg[88]. The electron densities for these two residues are unambiguous. Asp[75] is the third residue in a type II turn that connects the second and third β-strands of the subunit. Arg[88] is located near the 3′-phosphate group of the CoA ribose, and in fact, the peptidic NH group of Arg[89] lies within 2.8 Å of one of the phosphoryl oxygens. The torsional angles for Arg[88] are similar in the unbound enzyme structure (3).

All three structures described in this study are, like the structure of the unbound wild-type thioesterase, homotetramers with 16-kDa subunits. An α-carbon trace of the complete tetramer for the thioesterase complexed with 4-hydroxyphenacyl-CoA is depicted in Fig. 3. The quaternary structure can be aptly described as a dimer of dimers. The α-carbons for the enzymes complexed with either 4-hydroxyphenacyl-CoA or 4-hydroxybenzyl-CoA superimpose on those of the unbound wild-type thioesterase with root mean square deviations of 1.25 and 1.20 Å, respectively. Additionally, the α-carbons for the D17N mutant protein and the unbound wild-type enzyme superimpose with a root mean square deviation of 1.25 Å. On the other hand, the α-carbons for the complexes of the thioesterase with bound 4-hydroxyphenacyl-CoA or 4-hydroxybenzyl-CoA

TABLE I
X-ray data collection statistics

Complex	Resolution	Independent reflections	Completeness	Redundancy	Avg I/Avg σ(I)	$R_{sym}{}^a$
	Å		%			
Wild-type enzyme-4-hydroxyphenacyl-CoA	30.0–1.50	20,139	94.1	5.3	30.6	3.8
	1.55–1.50[b]	1,828	87.0	3.4	4.0	17.3
Wild-type enzyme-4-hydroxybenzyl-CoA	30.0–1.80	11,789	98.0	3.3	19.2	5.1
	1.88–1.80	1,352	91.2	2.3	2.7	26.1
D17N enzyme-4-hydroxybenzoyl-CoA	30.0–2.80	3,068	85.1	2.2	6.2	7.8
	2.93–2.80	349	77.6	1.6	2.5	28.5

[a] $R_{sym} = (\Sigma \mid I - \bar{I} \mid /\Sigma I) \times 100$.
[b] Statistics for the highest resolution bin.

TABLE II
Relevant refinement statistics

Complex	Thioesterase-4-hydroxyphenacyl-CoA	Thioesterase-4-hydroxybenzyl-CoA	D17N protein-4-hydroxybenzoyl-CoA
Resolution limits (Å)	30.0–1.50	30.0–1.80	30.0–2.80
R-factor (overall) percentage/no. of reflections[a]	16.3/20139	19.3/11789	14.8/3068
R-factor (working) percentage/no. of reflections	16.1/18125	19.2/10610	14.8/2761
R-factor (free) percentage/no. of reflections	19.8/2014	24.7/1179	24.7/307
No. of protein atoms	1136[b]	1127[c]	1122
No. of hetero-atoms	239[d]	167[e]	72[f]
Bond lengths (Å)	0.013	0.013	0.014
Bond angles (deg)	2.31	2.47	2.53
Trigonal planes (Å)	0.008	0.007	0.006
General planes (Å)	0.011	0.013	0.011
Torsional angles (deg)[g]	15.8	17.6	18.6

[a] R-factor $= (\Sigma|F_o - F_c|/\Sigma|F_o|) \times 100$, where F_o is the observed structure-factor amplitude and F_c is the calculated structure-factor amplitude.
[b] This value includes multiple conformations for Leu[31], Ser[67], Ser[99], Met[121], and Ser[141].
[c] This value includes multiple conformations for Glu[53].
[d] This value includes 173 water molecules, one 4-hydroxyphenacyl-CoA molecule, and two ethylene glycol moieties.
[e] This value includes 111 water molecules and one 4-hydroxybenzyl-CoA molecule.
[f] This value includes 15 water molecules and one 4-hydroxybenzoyl-CoA molecule.
[g] The torsional angles were not restrained during the refinement.

TABLE III
Wild-type and D17N mutant thioesterase-ligand binding constants measured at pH 7.5 and 25 °C

Inhibition constants (K_i) were calculated from steady-state competitive inhibition data, and dissociation constants (K_d) were calculated from protein fluorescence quenching data.

Complex	Binding constant
Wild-type enzyme-4-hydroxyphenacyl-CoA	$K_i = 1.4 \pm 0.1 \ \mu M$
Wild-type enzyme-4-hydroxybenzyl-CoA	$K_i = 0.26 \pm 0.02 \ \mu M$
Wild-type enzyme-4-hydroxyphenacyl-CoA	$K_d = 0.33 \pm 0.01 \ \mu M$
Wild-type enzyme-4-hydroxybenzyl-CoA	$K_d = 1.09 \pm 0.04 \ \mu M$
D17N enzyme-4-hydroxyphenacyl-CoA	$K_d = 0.42 \pm 0.02 \ \mu M$
D17N enzyme-4-hydroxybenzyl-CoA	$K_d = 1.00 \pm 0.05 \ \mu M$
D17N enzyme-4-hydroxybenzoyl-CoA	$K_d = 0.14 \pm 0.02 \ \mu M$

superimpose with a root mean square deviation of 0.20 Å. Clearly ligand binding influences the structure of the enzyme to some extent. The most significant regions of change upon ligand binding are concentrated in the loops defined by Arg[100]–Gln[108] and Asn[122]–Leu[127]. The latter loop is located near the pyrophosphate moiety of the respective inhibitor.

The active sites for the thioesterase are located at the interfaces of subunits A and B and subunits C and D (Fig. 3). As can be seen in Fig. 3, the thioester and pantetheine moieties are bound in a deep crevice formed at the subunit-subunit interface, whereas the nucleotide moiety is positioned in a depression located on the solvated surface of one of the paired subunits.

Structure of the Thioesterase-4-Hydroxyphenacyl-CoA Complex—The 4-hydroxyphenacyl inhibitor differs from the natural substrate by one methylene group positioned between the sulfur of the CoA and the carbonyl carbon of the acyl group (Scheme 2). A close-up view of the thioesterase active site with bound 4-hydroxyphenacyl is displayed in Fig. 4a. For the sake of clarity, only those residues located within 3.5 Å of the acyl pantetheine unit are shown. Trp[47] from one subunit and Trp[23] and Tyr[24] from the second subunit encircle the aromatic moiety of the ligand. Two aspartate residues lie near the 4-hydoxyphenacyl group, namely Asp[32] from one subunit and Asp[17] from the second subunit. These residues are separated by ~7 Å. Note that O[δ2] of Asp[17] is positioned at 3.2 Å from the carbonyl carbon of the phenacyl group. There are four well ordered water molecules located within 3.5 Å of the acyl pantetheine moiety, two of which serve to link the polar groups of the ligand to either N[ε1] of Trp[47] or O[η] of Tyr[27].

A cartoon of the hydrogen-bonding pattern exhibited between the ligand and the protein is presented in Fig. 4b. The ribose ring of the inhibitor is in the C[2']-*endo* configuration. Thirteen water molecules are located within hydrogen bonding distance to the ligand. There is an ethylene glycol molecule that serves as a bridge between one of the hydroxyl groups of the acyl pantetheine unit and a phosphoryl oxygen. Interestingly, only one protein side chain, namely that contributed by Ser[91], participates directly in ligand binding. All of the other interactions between the protein and the inhibitor are mediated through backbone peptidic NH groups, carbonyl oxygens, and/or solvents. Of interest is the fact that the three positively charge residues Arg[88], Arg[89], and Lys[90], which are in the vicinity of the CoA phosphate groups, are not used in ion pair formation. Rather the side chain of Lys[90] interacts with the inhibitor through a bridging water molecule. Likewise, the guanidinium group of Arg[88] lies within hydrogen bonding distance to a water, which, in turn, interacts with N-3 of the adenine ring.

Structure of the Thioesterase-4-Hydroxybenzyl-CoA Complex—In 4-hydroxybenzyl-CoA, the carbonyl moiety of the acyl group has been removed (Scheme 2). A close-up view of the thioesterase active site with this bound ligand is shown in Fig. 5a, and a superposition of the active sites with either bound

(a)

FIG. 2. **Coordinate quality for the 4-hydroxyphenacyl-CoA-thioesterase complex.** Shown in *a* is a Ramachandran plot for all nonglycinyl main chain dihedral angles. Those ϕ,ψ values fully allowed are enclosed by the *solid lines*, whereas those only partially allowed are encircled by the *dashed lines*. The electron density corresponding to the bound ligand is displayed in *b*. The map shown was calculated with coefficients of the form $F_o - F_c$, where F_o was the native structure factor amplitude and F_c was the calculated structure factor amplitude from the model lacking the coordinates for the ligand. The map was calculated to 1.5 Å resolution and contoured at 2.5 σ.

(b)
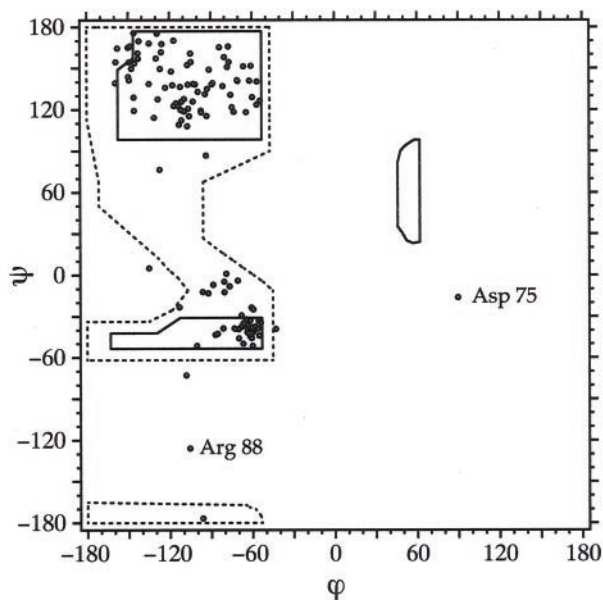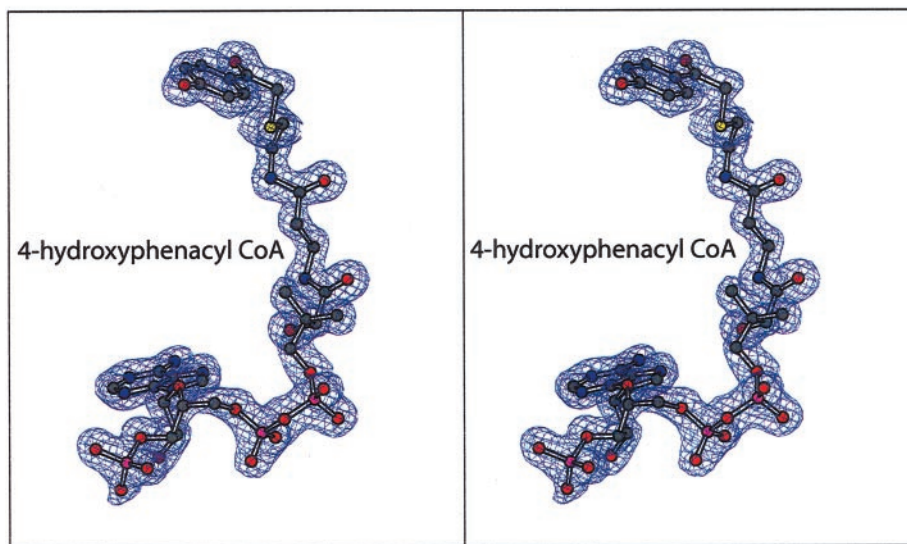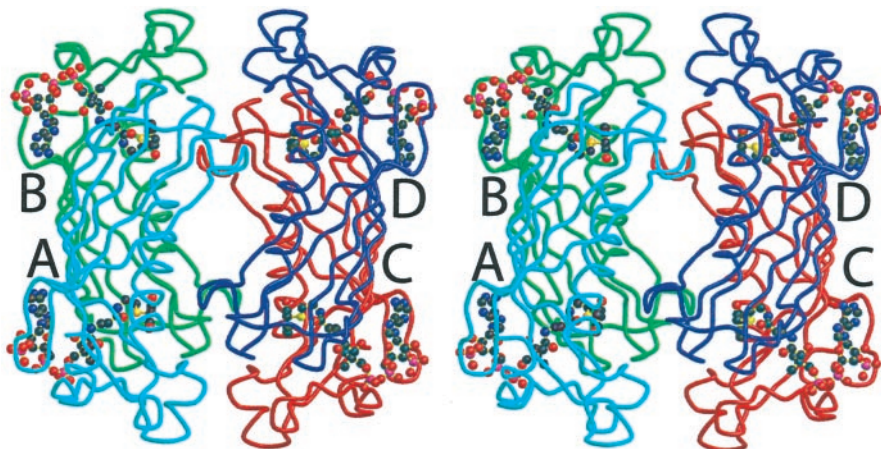
FIG. 3. **α-Carbon trace of the thioesterase tetramer.** The four subunits, all of which contain residues Ala[2]–Ser[141], are colored in *cyan*, *green*, *blue*, and *red*. The bound 4-hydroxyphenacyl-CoA ligands are drawn in *ball-and-stick* representations.
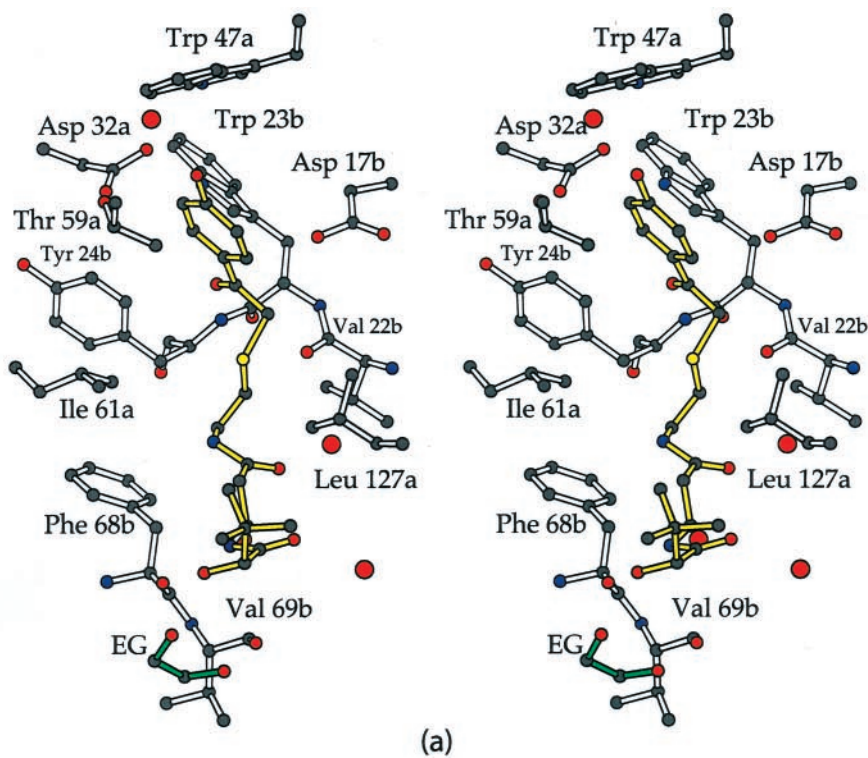
FIG. 4. **The thioesterase active site with bound 4-hydroxyphenacyl-CoA.** For the sake of clarity only those residues located within 3.5 Å of the acyl pantetheine unit are shown in *a*. The ligand is highlighted with *yellow bonds*. The "*a*" and "*b*" suffixes on the labels indicate residues from two different subunits. A cartoon of the hydrogen-bonding pattern exhibited between the protein and the ligand is displayed in *b*. The *dashed lines* indicate possible hydrogen bonding interactions within 3.2 Å.

4-hydroxybenzyl-CoA or 4-hydroxyphenacyl-CoA is given in Fig. 5*b*. In the case of 4-hydroxybenzyl-CoA, there are five ordered water molecules lying within 3.5 Å of the acyl pantetheine group. The ethylene glycol molecule discussed above is not observed in the model with bound 4-hydroxybenzyl-CoA. As can be seen in Fig. 5*b*, the aromatic moieties of both inhibitors occupy, within experimental error, identical positions within the thioesterase active site. The lack of the carbonyl group in 4-hydroxybenzyl-CoA, however, results in a movement of the ligand within the active site such that the positions of the
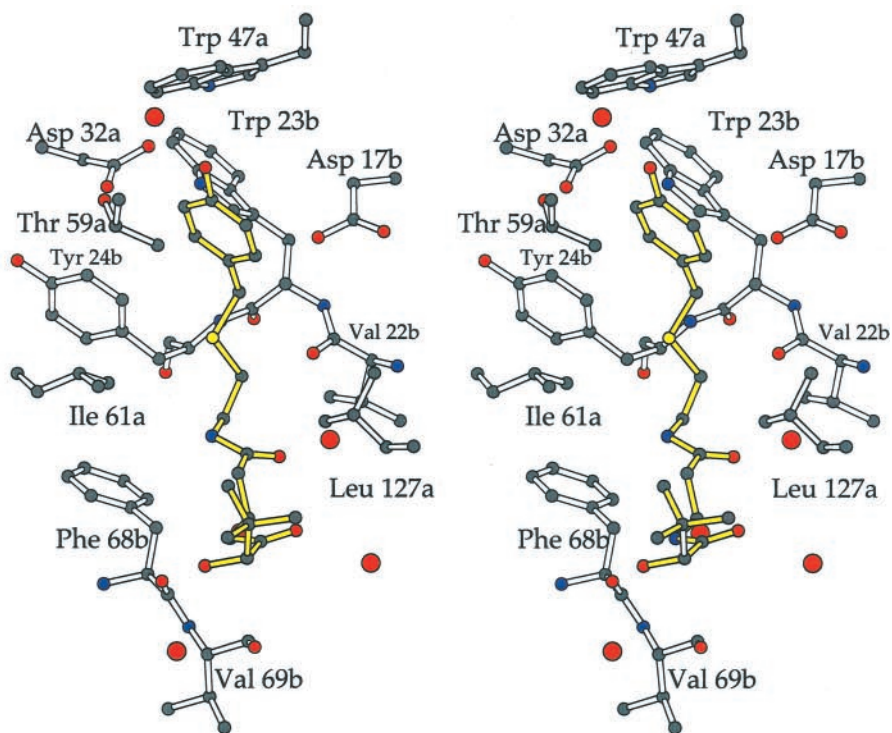
FIG. 5. **The thioesterase active site with bound 4-hydroxybenzyl-CoA.** For the sake of clarity only those residues located with 3.5 Å of the acyl pantetheine unit are shown in *a*. A superposition of the thioesterase active sites with bound 4-hydroxybenzyl-CoA (*red*) or 4-hydroxyphenacyl (*black*) is depicted in *b*.
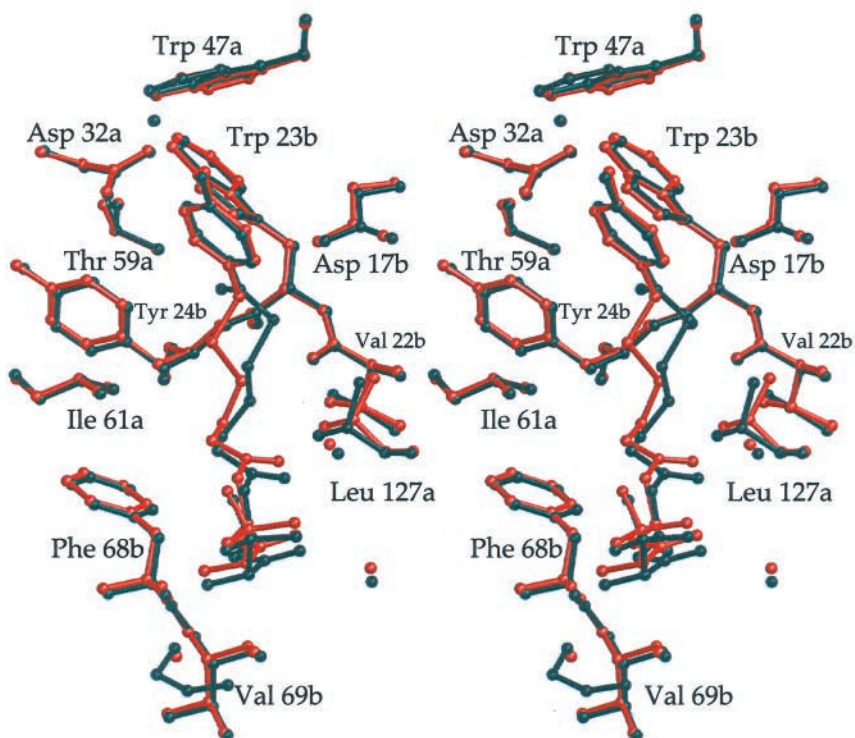
sulfurs in 4-hydroxybenzyl-CoA *versus* 4-hydroxyphenacyl-CoA differ by ~1.5 Å.

Possible Catalytic Mechanism for the Thioesterase—As ex-

pected, Asp[17] of the wild-type thioesterase and Asn[17] of the mutant protein coincide within experimental error. Because of the lower resolution of the x-ray data from the D17N mutant
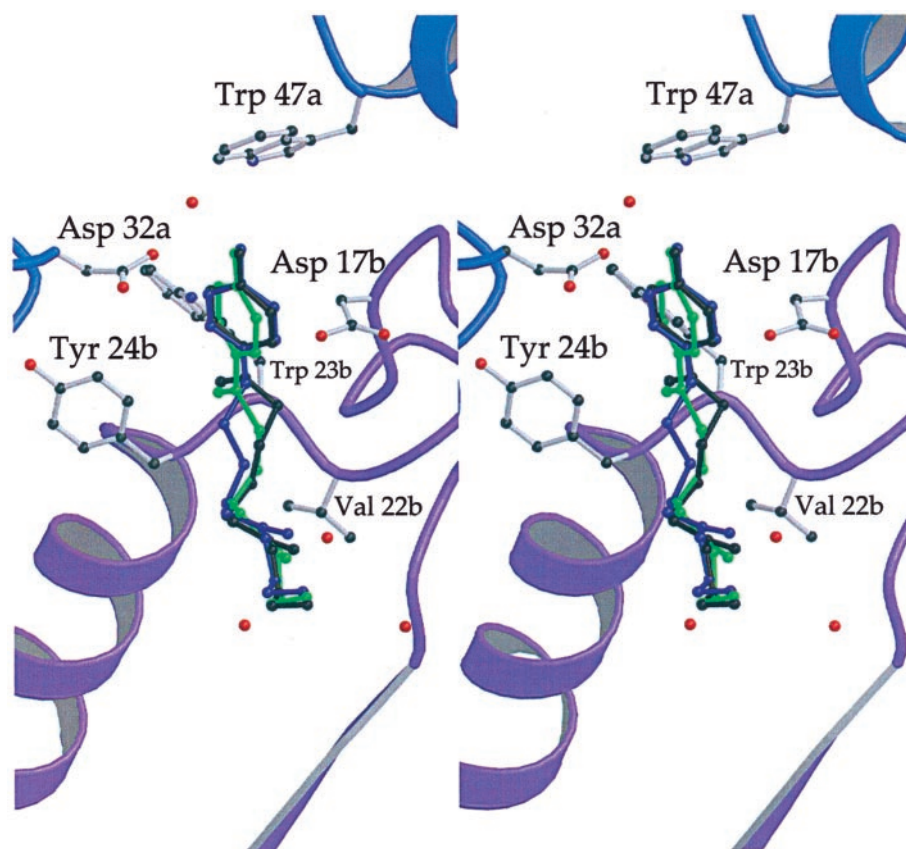
F<small>IG</small>. 6. **Superposition of the three ligands within the thioesterase active site.** The 4-hydroxyphenacyl-CoA, 4-hydroxybenzyl-CoA, and the 4-hydroxybenzoyl-CoA ligands are depicted in *black*, *blue*, and *green*, respectively.

protein crystals, however, it was not possible to define the solvent structure. Given that the three ligands are bound in the active site in approximately the same orientation as can be seen in Fig. 6, it is possible to discuss a catalytic mechanism for the thioesterase based on the arrangement of the groups in the enzyme-4-hydroxyphenacyl complex. The thioester carbonyl group is positioned at the N-terminal region of an active site helix, thereby placing the reaction center under the influence of a positive helical dipole moment. Specifically, this carbonyl group is locked into place via a hydrogen bond with the backbone peptidic NH group of Tyr[24] as indicated in Fig. 4*b*. Most likely the hydrogen bond and the helical dipole moment serve to polarize the electron density away from the carbonyl carbon, thereby making it more susceptible to nucleophilic attack. Additionally, the C-4 OH group on the ring of the inhibitor (or substrate) serves to correctly position the ligand into the active site by forming hydrogen bonds with the backbone peptidic NH of Thr[59] and a water molecule that is in turn hydrogen-bonded to $N^{\epsilon 1}$ of Trp[47].

Thus far, all biochemical and structural data indicate that the catalytic residue in this thioesterase is Asp[17]. The side chain of Asp[17] is held into position through a hydrogen bonding interaction with the backbone peptidic NH group of Ala[19]. In the wild-type enzyme complexed with 4-hydroxyphenacyl-CoA, the Asp[17] oxygen is ~3.2 Å away from the carbonyl carbon, whereas in the D17N mutant protein complexed with 4-hydroxybenzoyl-CoA, $N^{\delta 2}$ of Asn[17] is positioned at ~3.7 Å from the carbonyl carbon. It was originally speculated that Asp[17] would be involved in activating a water molecule for attack on the thioester carbonyl carbon (3). On the basis of the current structural data, however, there is apparently not enough space between the ligand and Asp[17] to accommodate a water molecule. Indeed, there are no water molecules bound in the region between the Asp[17] carboxylate side chain and either the 4-hydroxybenzyl-CoA or 4-hydroxyphenacyl-CoA inhibitors. Sol-

vent accessibility calculations with a search probe of 1.4 Å further support an active site devoid of waters between Asp[17] and the inhibitors or substrate (14).

The distance of the nucleophile from the carbonyl carbon and its attack angle (15), coupled with the absence of a water molecule near the reaction center, suggests the possibility that Asp[17] functions as a nucleophile in the hydrolysis of 4-hydroxybenzoyl-CoA rather than as a general base. Nucleophilic catalysis requires that the reaction proceeds via an anhydride enzyme intermediate. Catalysis by phosphotransferases of the haloalkanoic acid dehalogenase enzyme family is known to proceed via aspartylphosphate intermediates (16–20). Moreover, the catalytic mechanisms of succinyl-5CoA:3-ketoacid CoA-transferase (21, 22) and glutaconate CoA-transferase (23, 24) proceed via acyl transfer to an active site glutamate to form an anhydride intermediate, which subsequently reacts with the displaced CoA to form the glutamyl-CoA thioester intermediate. The formation of the aspartyl 4-hydroxybenzoate intermediate during 4-hydroxybenzoyl-CoA thioesterase catalysis has, therefore, ample precedence.

According to the present structural data, the active site does not offer acid catalysis for stabilization of the displaced CoA thiolate anion. On the other hand, the basicity of this anion is very modest (conjugate acid pK_a = ~8.5), and electrostatic interactions between it and the positive end of the helix dipole may be all the stabilization that is required. If the reaction proceeds via an acylated enzyme intermediate, then it would be expected that once the CoA departs, the water nucleophile binds and attacks at the carbonyl carbon. The identity of the base required to position and activate the water for nucleophilic attack is unknown at the present time.

In summary, the present study defines in detail the interactions required for the binding and positioning of a substrate molecule within the active site pocket of 4-hydroxybenzoyl-CoA thioesterase. Several key and intriguing questions remain for

future study. For example, does the reaction proceed via simple base catalyzed hydrolysis or via nucleophilic catalysis? If the former occurs, where does the water molecule bind? If the latter situation is operational, how is the water molecule activated for hydrolysis of the acylated enzyme intermediate? If the reaction occurs via a covalent enzyme intermediate, is the nucleophilic displacement concerted? Both biochemical and x-ray crystallographic experiments designed to address these issues are presently underway.

REFERENCES

1. Klages, U., Markus, A., and Lingens, F. (1981) *J. Bacteriol.* **146**, 64–68
2. Dunaway-Mariano, D., and Babbitt, P. C. (1994) *Biodegradation* **5,** 259–276
3. Benning, M. M., Wesenberg, G., Liu, R., Taylor, K. L., Dunaway-Mariano, D., and Holden, H. M. (1998) *J. Biol. Chem.* **273,** 33572–33579
4. Leesong, M., Henderson, B. S., Gillig, J. R., Schwab, J. M., and Smith J. L. (1996) *Structure* **4,** 253–264
5. Li, J., Derewenda, U., Dauter, Z., Smith, S., and Derewenda, Z. S. (2000) *Nat. Struct. Biol.* **7,** 555–559
6. Kraulis, P. J. (1991) *J. Appl Crystallogr.* **24,** 946–950
7. Chang, K.-H., Liang, P.-H., Beck, W., Scholten, J. D., and Dunaway-Mariano, D. (1992) *Biochemistry* **31,** 5606–5610
8. Otwinowski, Z., and Minor, W. (1997) *Methods Enzymol.* **276,** 307–326
9. Navaza, J. (1994) *Acta Crystallogr. Sect. A* **50,** 157–163
10. Tronrud, D. E., Ten Eyck, L. F., and Matthews, B. W. (1987) *Acta Crystallogr. Sect. A* **43**, 489–501
11. Roussel, A., and Cambillau, C. (1991) *Silicon Graphics Geometry Partners Directory*, Silicon Graphics, Mountain View, CA
12. Luo, L., Taylor, K. L., Xiang, H., Wei, Y., Zhang, W., and Dunaway-Mariano D. (2001) *Biochemistry* **40,** 15684–15692
13. Anderson, K. S., Sikorski, J. A., and Johnson, K. A. (1988) *Biochemistry* **27,** 1604–1610
14. Kleywegt, G. J., and Jones, T. A. (1994) *Acta Crystallogr. Sect. D Biol. Crystallogr.* **50**, 178–185
15. Lightstone, F. C., and Bruice, T. C. (1996) *J. Am. Chem. Soc.,* **118,** 2595–2605
16. Cantley, L. C., Jr., Cantley, L. G., and Josephson, L. (1978) *J. Biol. Chem.* **253,** 7361–7368
17. Missiaen, L., Wuytack, F., De Smedt, H., Vrolix, M., and Casteels, R. (1988) *Biochem. J.* **253,** 827–833
18. Murphy, A. J., and Coll, R. J. (1993) *J. Biol. Chem.* **268,** 23307–23310
19. Pick, U. (1982) *J. Biol. Chem.* **257,** 6111–6119
20. Troullier, A., Girardet, J. L., and Dupont, Y. (1992) *J. Biol. Chem.* **267,** 22821–22829
21. Solomon, F., and Jencks, W. P. (1969) *J. Biol. Chem.* **244,** 1079–1081
22. Rochet, J.-C., and Bridger, W. A. (1994) *Protein Sci.* **3,** 975–981
23. Mack M., and Buckel, W. (1997) *FEBS Lett.* **405,** 209–212
24. Jacob, U., Mack, M., Clausen, T., Huber, R., Buckel, W., and Messerschmidt, A. (1997) *Structure* **5,** 415–426